Mixed Valency in Binuclear Cyano-Bridged Manganese Bis(carbonyl) Complexes and Stereochemical Control of Their Oxidation. A Molecular Orbital Study

Gabino A. Carriedo,*,† Neil G. Connelly,‡ Santiago Alvarez,*,§ Enrique Pérez-Carreño,∥ and Santiago García-Granda‡

Departamento de Química Organometálica and Departamento de Química Física y Analítica, Universidad de Oviedo, Oviedo, Spain, School of Chemistry, University of Bristol, Bristol BS8 1TS, U.K., and Departament de Química Inorgànica, Universitat de Barcelona, Barcelona, Spain

Received April 16, 1992

Molecular orbital calculations at the extended Hückel level have been carried out on the model binuclear cyano-bridged cationic complexes of the type $\{[Mn]-CN-[Mn]\}^+$, where [Mn] = *cis*- or *trans-mer*-$Mn(CO)_2(PH_3)_3^+$. The results are consistent with a weak Mn- - -Mn interaction mediated by the CN bridge. The energy and composition of the highest occupied orbitals are determined by the stereochemistry and so is the Mn atom at which the HOMO is localized. A good correlation is found between these data and the experimental electrode potentials and the effects of the ancillary ligands corresponding to the real complexes with [Mn] = *cis*- or *trans-mer*-$Mn(CO)_2$(diphos)L (diphos = dppm or dppe, L = PR_3 or $P(OR)_3$). An explanation is also found for the fact that the oxidatively induced isomerization of the *cis*-$Mn(CO)_2$ fragments occurs even when the oxidation is centered at the other Mn center. The calculations also indicate that the dications formed upon the first oxidation can be considered as very weakly coupled class II mixed-valence complexes, with a different degree of electron delocalization depending on the stereochemistry of the $Mn(CO)_2L_3$ fragments bridged by the cyanide ligand.

The importance of electron-transfer (ET) processes[1] has promoted an increasing interest in the synthesis and the electrochemistry of polymetallic complexes having two or more metal atoms connected through a bridging ligand.[2,3] Due to its electronic characteristics, the bridging cyanide (CN) ligand has been the subject of many recent studies,[4] especially in the examination of intramolecular energy-transfer processes.[5]

Molecular orbital calculations at different levels of sophistication are highly valuable for the understanding of ET processes[6] and for analyzing the electronic structure of binuclear mixed-valence complexes with different types of bridging ligands,[2,7] as well as their stability.[8]

Recently we showed that the results of the chemical and electrochemical oxidation of several CN-bridged binuclear Mn[9] and Mn and Fe[10] complexes of the types $\{[Mn]-(\mu\text{-}CN)-[Mn]\}^+$ and $\{[Mn]-(\mu\text{-}CN)-[Fe]\}^+$, where [Mn] = *cis*- or *trans-mer*-$Mn(CO)_2$(diphos)$[P(OR)_3]$ and [Fe] = Fe(diphos)(η-C_5H_5) (diphos = diphosphine), indicate that there may be some electronic interaction between the two metal centers. In order to examine the nature of this interaction in more detail, we have carried out an extended Hückel molecular orbital study on the model binuclear $\{[Mn]-CN-[Mn]\}^+$ complexes where [Mn] = *cis* or *trans-mer*-$Mn(CO)_2(PH_3)_3$. In this paper we describe the results of these calculations and discuss the stereochemical control of the oxidation of binuclear CN-bridged manganese carbonyl cationic compounds in terms of their electronic structure.

Computational Details

Extended Hückel molecular orbital calculations[11] were carried out on the model binuclear CN-bridged complexes **1–5** with an eclipsed conformation, as represented in Figure 1, and using the modified Wolfsberg–Helmholz formula.[12] The atomic parameters used for C, O, H, and P were the standard ones, while those for Mn were taken from the literature.[13] The averages of chemically equivalent bond distances from the experimental structure of the cyanide-bridged complex $\{[Mn(CO)_3(phen)]_2(\mu\text{-}CN)\}PF_6$ (phen = phenanthroline)[14] were used in our calculations: Mn–N(cyanide) = 2.064, Mn–C(cyanide) = 2.004, Mn–C(carbonyl) = 1.810, and C–O = 1.135 Å. In our structural model we substituted phen groups for the PH_3 groups with bond distances[15] Mn–P = 2.305 and P–H = 1.435 Å, and for the asymmetric complex we used $P(OH)_3$ with bond distances Mn–P = 2.216, P–O = 1.595, and O–H = 0.967 Å. The angles around the manganese atoms were those of an idealized octahedral configuration, and the angles of the $-PH_3$ ligands were those of the tetrahedral geometry. The calculations were carried out on a Micro VAX 3400 computer at the Scientific Computer Center of the University of Oviedo, with a locally modified version of the program ICON.

Frontier Orbitals of the $[L_3(CO)_2Mn(\mu\text{-}CN)Mn(CO)_2L_3]^+$ Isomers

The nature and energy ordering of the frontier orbitals of several geometrical isomers of the $[L_3(CO)_2Mn(\mu\text{-}CN)Mn(CO)_2L_3]^+$ ion (**1–5**, Figure 1), obtained in our MO calculations, can be

† Departamento de Química Organometálica, Universidad de Oviedo.
‡ University of Bristol.
§ Universitat de Barcelona.
∥ Departamento de Química Física y Analítica, Universidad de Oviedo.

(1) For a number of references see: MacQueen, D. B.; Schanze, K. S. *J. Am. Chem. Soc.* **1991**, *113*, 7470.
(2) Creutz, C. *Prog. Inorg. Chem.* **1983**, *30*, 1.
(3) Geiger, W. E.; Connelly, N. G. *Adv. Organomet. Chem.* **1985**, *24*, 87.
(4) Oswald, B.; Powell, A. K.; Rashwan, F.; Heinze, J.; Vahrenkamp, H. *Chem. Ber.* **1990**, *123*, 243 and references therein. Bell, A.; Lippard, S. J.; Roberts, M.; Walton, R. A. *Organometallics* **1983**, *2*, 1562.
(5) Zhou, B.; Pfennig, W.; Steiger, J.; Van Engen, D.; Bocarsly, A. B. *Inorg. Chem.* **1990**, *29*, 2456 and references therein. Doorn, S. K.; Hupp, J. T. *J. Am. Chem. Soc.* **1989**, *111*, 1142. Vogler, A.; Kunkely, H. *Inorg. Chim. Acta* **1988**, *150*, 1. Lei, Y.; Buranda, T.; Endicott, J. F. *J. Am. Chem. Soc.* **1990**, *112*, 8820.
(6) Burdett, J. K. *Comments Inorg. Chem.* **1981**, *1*, 85 and references therein.
(7) Lauher, J. W. *Inorg. Chim. Acta* **1980**, *39*, 119. Zhang, L.-T.; Ko, J.; Ondrechen, M. J. *J. Am. Chem. Soc.* **1987**, *109*, 1666, 1672. Gross-Lannert, R.; Kaim, W.; Olbrich-Deussner, B. *Inorg. Chem.* **1990**, *29*, 5046. Reimers, J. R.; Hush, N. S. *Inorg. Chem.* **1990**, *29*, 4510.
(8) Kaim, W.; Kasack, V. *Inorg. Chem.* **1990**, *29*, 4696.
(9) Carriedo, G. A.; Connelly, N. G.; Crespo, M. C.; Quarmby, I. C.; Riera, V.; Worth, G. H. *J. Chem. Soc., Dalton Trans.* **1991**, 315.
(10) Barrado, G.; Carriedo, G. A.; Díaz-Valenzuela, C.; Riera, V. *Inorg. Chem.* **1991**, *30*, 4416.
(11) Hoffmann, R. *J. Chem. Phys.* **1963**, *39*, 1397.
(12) Ammeter, J. H.; Bürgi, H.-B.; Thibeault, J. C.; Hoffmann, R. *J. Am. Chem. Soc.* **1978**, *100*, 3686.
(13) Elian, M.; Hoffman, R. *Inorg. Chem.* **1975**, *14*, 1058.
(14) Carriedo, G. A.; Crespo, M. C.; Riera, V.; Valin, M. L.; Moreiras, D.; Solans, X. *Inorg. Chim. Acta* **1986**, *121*, 191.
(15) Allen, F. H.; Kennard, O.; Watson, D. G.; Brammer, L.; Orpen, A. G.; Taylor, R. *J. Chem. Soc., Perkin Trans. 2* **1987**, S1.

0020-1669/93/1332-0272$04.00/0

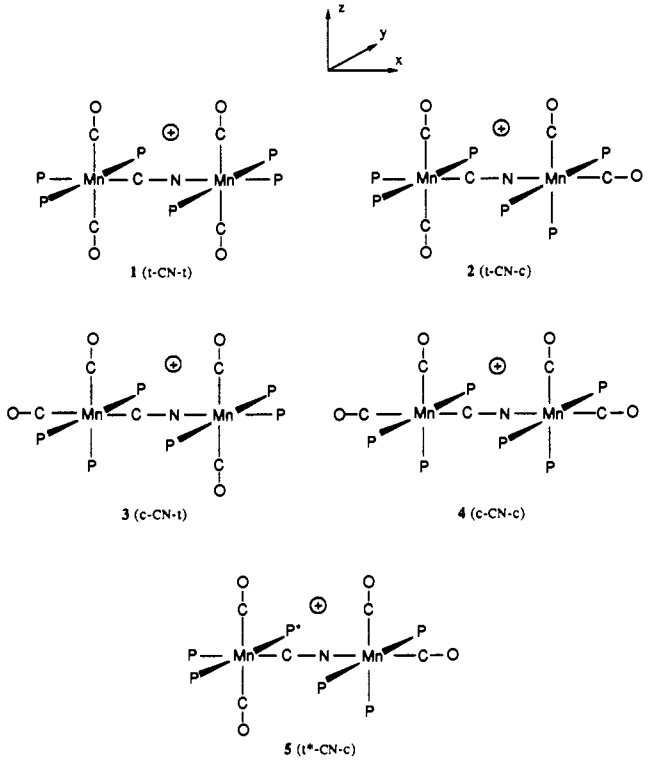

Figure 1. Model compounds used in our molecular orbital calculations. P represents PH_3, and P* is $P(OH)_3$.

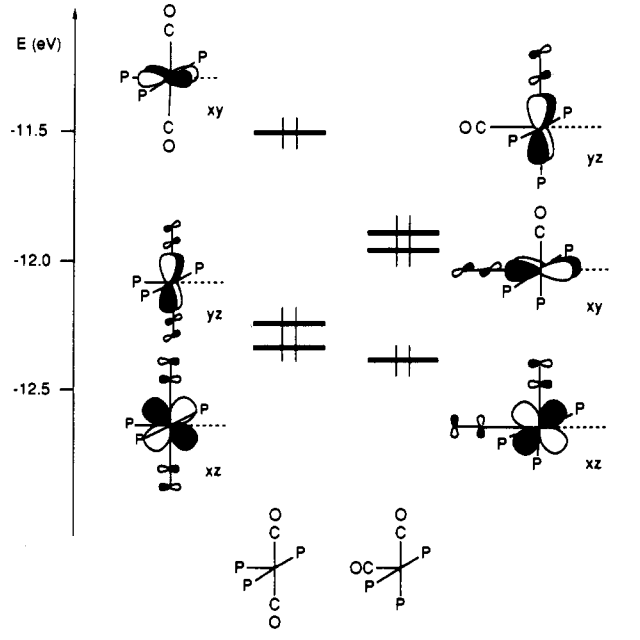

Figure 2. Frontier orbitals (t_{2g}-like block) of the (left) *trans*- and (right) *cis*-$[Mn(PH_3)_3(CO)_2]^+$ fragments. The coordinate system is as in Figure 1.

easily understood by building them up stepwise from the orbitals of the $Mn(CO)_2L_3^+$ fragments and the cyanide ion.

The uppermost occupied orbitals of the *cis*- and *trans*-$Mn(CO)_2L_3^+$ fragments, shown in Figure 2, can be described as a pseudo-t_{2g} set of an octahedral fragment,[16] Mn–P nonbonding and Mn–CO π bonding. Their energies differ because of the different interactions with the empty π^* orbitals of the CO ligands: d_{xz} and d_{yz} of the trans fragment, as well as d_{xz} of the cis fragment (labeled *xz*, *yz*, and *xy*, respectively, from now on),

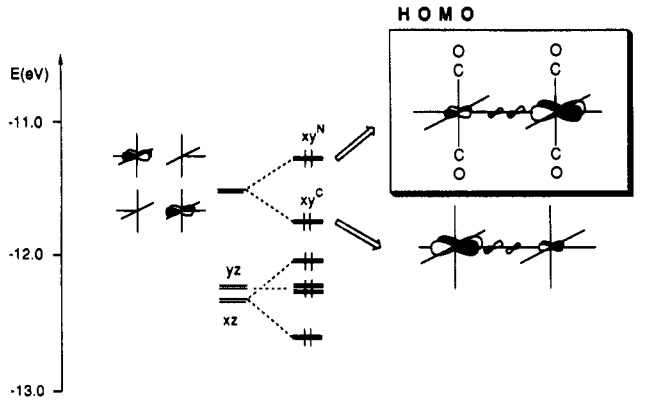

Figure 3. Splitting of the t_{2g}-like orbitals of two *trans*-$[Mn(PH_3)_3(CO)_2]^+$ fragments upon interaction with the π orbitals of the bridging cyano ligand in the model compound **1**. The N of the CN bridge is the atom bonded to the Mn on the right.

interact with two CO ligands and appear at lower energy; *xy* and *yz* of the cis fragment interact with only one carbonyl ligand each and are less stabilized, and finally, *xy* of the trans fragment does not interact at all with CO and is the highest occupied orbital. Let us stress that the relative energies of the pseudo-t_{2g} orbitals are only determined by the π-acid character of the CO ligands and the number of d/π^* interactions and are therefore independent of the approximations involved in the extended Hückel methodology. These results are consistent with the qualitative[17] and quantitative[18] analysis of the bonding in mononuclear octahedral dicarbonyl complexes and with other calculations carried out by us on $[Mn(CN)(CO)_2(PH_3)_3]$ complexes.[19]

Even if some direct d–d interaction between the two Mn atoms could have been expected in the case of the short CN bridging ligand,[2] the values for the corresponding overlap integrals are zero at the Mn- - -Mn distance (5.175 Å) used in the calculations (the Mn- - -Mn distance[14] in the compound $\{[fac\text{-}Mn(CO)_3(phen)]_2(\mu\text{-}CN)\}PF_6$ is 5.2 Å). If we let the pseudo-t_{2g} orbitals of the two Mn centers interact with the π orbitals of the bridging cyanide, we must pay attention to only *xy* and *xz* orbitals, the ones directed toward the bridging region. Let us take as an example the model compound with a trans geometry at both Mn atoms (molecule **1**) for which a simplified interaction diagram is shown in Figure 3, where the size of the lobes of each contributing atomic orbital is roughly proportional to its corresponding electron population obtained from a Mulliken analysis. A combination of the *xy* orbitals of the two Mn atoms interacts with the π_y^* orbital of CN and is therefore stabilized. Another combination of such d orbitals interacts with the occupied π_y orbital of CN and is consequently destabilized, becoming the HOMO of the binuclear compound. A similar splitting pattern results for the *xz* orbitals (Figure 3). Considering the different orbital ordering of the cis fragment (Figure 2), the interaction diagrams for the remaining model compounds (Figures 4–6) can be easily understood. In all cases, the orbital composition of the HOMO indicates that there is a weak interaction between the two manganese atoms mediated by the CN bridge. The resulting energies of the HOMO of each model compound are shown in Table I and will be discussed later in regard to the redox potentials corresponding to the oxidation of the real complexes.

For the purpose of the present work, it is of the utmost importance to analyze the localization of the HOMO's of the different isomers. In Table I we present the electron populations of the HOMO's associated with the *xy* and *xz* atomic orbitals,

(16) Albright, T.; Burdett, J. K.; Whangbo, M.-H. *Orbital* Interactions in Chemistry; J. Wiley: New York, 1985.

(17) Wimmer, F. L.; Snow, M. R.; Bond, A. M. *Inorg. Chem.* **1974**, *13*, 1617. Bursten, B. E. *J. Am. Chem. Soc.* **1982**, *104*, 1299 (see also: Bursten, B. E.; Darensbourg, D. J.; Kellog, G. E.; Lichtenberger, D. L. *Inorg. Chem.* **1984**, *23*, 4361).

(18) Mingos, D. M. P. *J. Organomet. Chem.* **1979**, *179*, C29.

(19) Carriedo, G. A.; Perez-Carreño, E. Unpublished results.

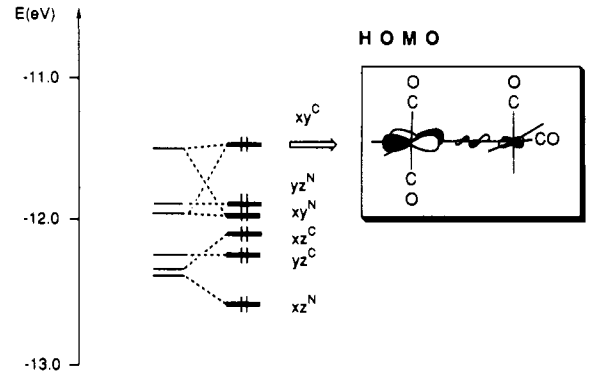

Figure 4. Splitting of the t_{2g}-like orbitals of one *trans*- and one *cis*-$[Mn(PH_3)_3(CO)_2]^+$ fragment upon interaction with the π orbitals of the bridging cyano ligand in the model compound **2**. The N of the CN bridge is the atom bonded to the Mn on the right.

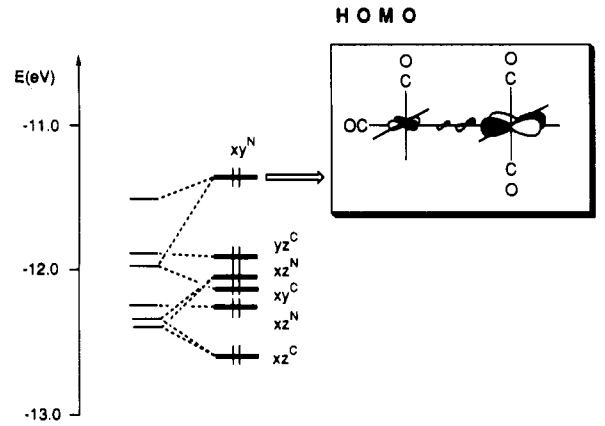

Figure 5. Splitting of the t_{2g}-like orbitals of one *cis*- and one *trans*-$[Mn(PH_3)_3(CO)_2]^+$ fragment upon interaction with the π orbitals of the bridging cyano ligand in the model compound **3**. The N of the CN bridge is the atom bonded to the Mn on the right.

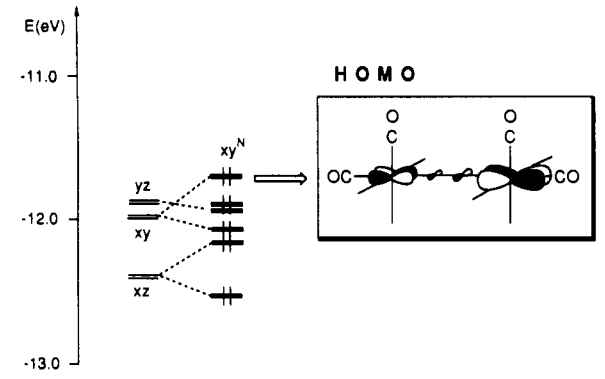

Figure 6. Splitting of the t_{2g}-like orbitals of two *cis*-$[Mn(PH_3)_3(CO)_2]^+$ fragments upon interaction with the π orbitals of the bridging cyano ligand in the model compound **4**. The N of the CN bridge is the atom bonded to the Mn on the right.

as obtained from a Mulliken population analysis. There it can be seen that such orbitals are spread throughout the two Mn centers, but with a larger localization on the one with a trans geometry. For molecules **1** and **4**, in which the two fragments have the same geometry, the HOMO is mostly localized on the N-bound metal atom. Therefore the lowest degree of delocalization corresponds to the cis–CN–trans isomer **3**. The preferential localization of the HOMO's on the trans fragments is a direct consequence of the higher energy of the *xy* orbital in that geometry as discussed above (Figure 2). On the other hand, when both $[Mn(CO)_2L_3]^+$ fragments present the same geometry, the asymmetry of the bridging ligand becomes relevant. Since the π orbital of CN is mostly localized on the nitrogen atom because of its greater electronegativity, it interacts mainly with

Table I. Orbital Energy and Main d-Orbital Contributions (Charge Matrix Elements) to the HOMO's of the Binuclear Complexes **1–5** (Figure 1)[a]

complex	ϵ (eV)	xy^C	xy^N	xz^C	xz^N
1 (trans–trans)	−11.28	0.573	**1.213**	0.000	0.000
2 (trans–cis)	−11.47	**1.268**	0.368	0.000	0.016
3 (cis–trans)	−11.36	0.149	**1.584**	0.006	0.000
4 (cis–cis)	−11.69	0.428	**0.910**	0.036	0.073
5 (trans*–cis)	−11.50	**1.204**	0.419	0.000	0.017

[a] The major contribution to each HOMO is boldface. The superindexes C and N refer to the atomic orbitals of the Mn atom at the C and N ends of the cyano bridge, respectively.

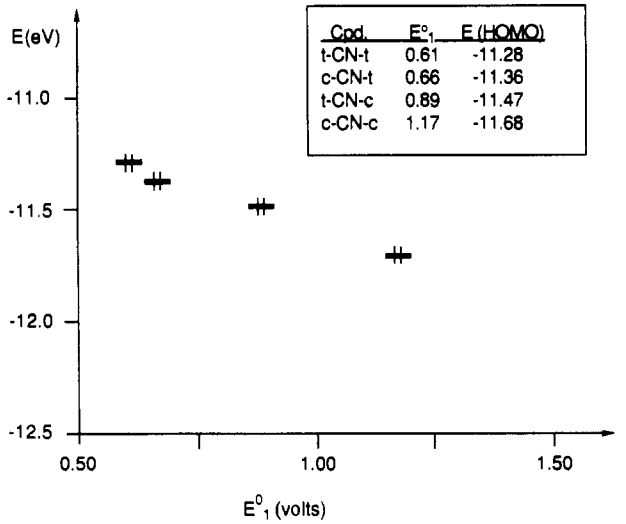

Figure 7. Energies of the highest occupied molecular orbitals of model compounds **1–4** plotted as a function of the first oxidation potentials of the corresponding geometrical isomers of the complexes $\{[P(OPh)_3](dppm)(CO)_2Mn–CN–Mn[P(OPh)_3](dppm)(CO)_2\}^+$. The potentials were measured in CH_2Cl_2 with reference to SCE (see ref 9).

the xy^N orbital rather than with the in-phase combinations of the two *xy* orbitals, and the opposite happens with the π^* orbital of the CN, resulting in a HOMO localized at the N-side of the binuclear molecule.

Orbital Control of the Electrode Potentials

This simple analysis of the HOMO's of the model compounds **1–5** provides a basis for understanding the chemical and electrochemical oxidation of the monocationic binuclear cyano-bridged manganese carbonyl complexes to the corresponding di- and trications and the trends observed in their redox potentials.[9] In all the following discussion it should be borne in mind that the solvation effects that take place in solution during the oxidation of the real complexes have been neglected. It is well-known that the solvent plays an important role in the electrode potentials of the redox couples and in the relative stability of the different isomers, but in addition, the solvent also affects the electronic properties of the ligand-bridged mixed-valence complexes.[20] We have considered that those effects should be very similar for all the isomers in our study or, at least, that the existing differences are not sufficiently pronounced to affect significantly our conclusions. In a first approximation, the relative values of the first electrode potentials for the different isomers (**1–4**) are expected to depend on the energies of the corresponding HOMO's. In Figure 7 we present the energies of the t_{2g} orbitals of the model compounds **1–4** as a function of the experimental potentials of the corresponding geometric isomers with L = L′ = $P(OPh)_3$ and L-L = L′-L′ = dppm. A nice correlation is found between the electrode potential of the first oxidation of each complex ($E°_1$)

(20) See, for example: Hupp, J. T. *J. Am. Chem. Soc.* **1990**, *112*, 1563 and other references given in ref 1.

and the energy of the corresponding HOMO. Let us recall that the energy of the HOMO is essentially determined by the stereochemistry of the $Mn(CO)_2L_3^+$ fragments. Hence, the highest HOMO and the lower redox potential are those of complex **1**, which has two trans fragments, and the lowest HOMO and highest redox potential are those of complex **4**, having two cis fragments.

The second oxidation can in principle remove the second electron from the HOMO (**6**), thus producing a singlet state, or from the next occupied orbital (**7**), resulting in a triplet state. Given the

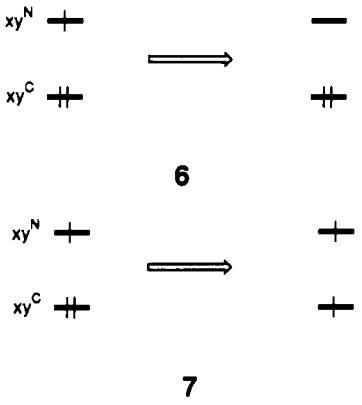

small energy difference between the two highest occupied orbitals, the triplet state is expected to be more stable than the singlet one, and it is likely that the second oxidation step proceeds as in **7** (because of the instability of the tricationic binuclear complexes, it was not possible to measure their magnetic moments to confirm experimentally this conclusion). On the other hand, due to the localization of the molecular orbitals, process **6** would imply the formation of a Mn^{I}–Mn^{III} compound, whereas oxidation as in **7** corresponds to the formation of a Mn^{II}–Mn^{II} complex. The second case agrees with the fact that the electrode potential for the first oxidation of the complexes is affected by changes in the ligands of one Mn site, whereas the potential for the second oxidation is affected by changes in the ligands of the other site. If the second oxidation proceeds as in **7**, the second electrode potentials should follow the order of the second occupied orbitals. This is what is found for the family of compounds with L = L′ = $P(OPh)_3$ and L-L = L′-L′ = dppm, as shown in Figure 8, where the first and second potentials are represented as a function of the corresponding orbitals. Considering all the analogous compounds studied previously by cyclic voltammetry, those having L,L′ = $P(OR)_3$ and L-L, L′-L′ = bidentate diphosphine, their first two electrode potentials (28 experimental data) are roughly linearly related to the energies of the two highest occupied orbitals of the corresponding model compounds. Deviations from linearity can be attributed to the presence of different ligands since each family of geometrical isomers bearing the same ligands shows a good correlation (the worst regression coefficient of three families with at least four data sets is 0.97).

Removal of the electron from the complex increases the net charges of the two manganese atoms but, because of the different degree of localization of the HOMO at each fragment, the charge increase is larger in one of them (see Table II). As an example, the data in Table II show that, in the case of the species [cis–CN–trans], the oxidation of the trans-Mn is almost unnoticed by the cis-Mn. It is thus clear that the first oxidation of each complex takes place mainly at one or another metal center depending on the stereochemistry (preferential oxidation of a trans site relative to a cis one) and on their positions relative to the CN bridge (N-bonded sites are more readily oxidized than C-bonded sites with the same stereochemistry). The detailed analysis of the cyclic voltammetry data, the CO stretching frequencies, and ESR data allowed us to establish at which Mn atom occurs the first

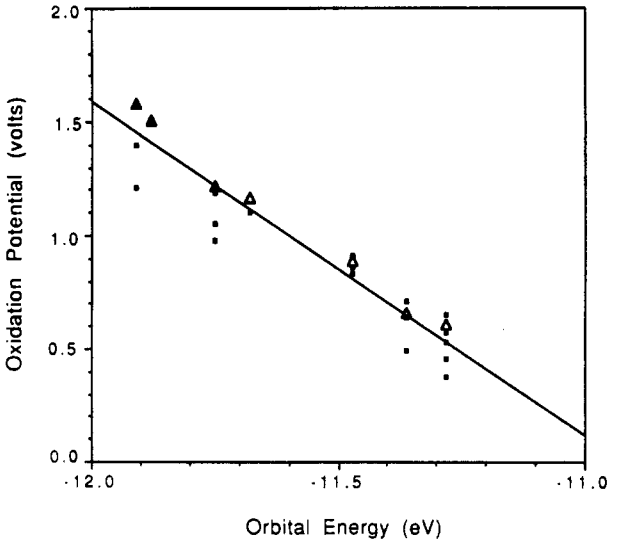

Figure 8. Plot of the first and second oxidation potentials[9] of the geometrical isomers of the cations $[L(L\text{-}L)(CO)_2Mn\text{–}CN\text{–}Mn(CO)_2L'\text{-}(L'\text{-}L')]^+$ as a function of the calculated orbital energy of the HOMO and second occupied orbital, respectively, of the model compounds **1**–**4**. The triangles correspond to the family with L = L′ = $P(OPh)_3$ and L-L = L′-L′ = dppm, and the squares to other compounds with L, L′ = $P(OR)_3$ and L-L, L′-L′ = diphosphine. The line shown is the least-squares fit of the 28 experimental data set ($E^\circ_i = -15.66 - 1.44\mathcal{E}_i$, where $\mathcal{E}_i$ is the orbital energy; regression coefficient = 0.92).

Table II. Calculated Net Atomic Charges

cation		Mn^C	C(CN)	N(CN)	Mn^N
[trans–CN–trans]$^+$	**1**	–0.235	0.144	–0.629	–0.227
[trans–CN–trans]$^{2+}$		0.051	0.155	–0.592	0.380
[trans–CN–cis]$^+$	**2**	–0.232	0.155	–0.662	–0.060
[trans–CN–cis]$^{2+}$		0.402	0.155	–0.598	0.132
[cis–CN–trans]$^+$	**3**	–0.122	0.114	–0.618	–0.224
[cis–CN–trans]$^{2+}$		–0.044	0.142	–0.599	0.568
[cis–CN–cis]$^+$	**4**	–0.121	0.125	–0.652	–0.060
[cis–CN–cis]$^{2+}$		0.112	0.138	–0.609	0.432
[trans*–CN–cis]$^+$	**5**	–0.250	0.153	–0.665	–0.060
[trans*–CN–cis]$^{2+}$		0.352	0.153	–0.602	0.159

oxidation for each binuclear compound,[9] in full agreement with the orbital picture presented above. The theoretical prediction that the oxidation of the binuclear complexes is preferentially located on one of the Mn centers, but also noted by the other, is also in agreement with the observation[9] that the first electrode potential (E°_1) is highly dependent on the monodentate phosphorus donor ligand L attached to the $Mn(CO)_2$(diphos)L fragment being oxidized and only slightly (but noticeably) dependent on the nature of the fragment at the other side of the bridge (stereochemistry and ligand L). This is another example of the use of different ligands at the two sides of bimetallic ligand-bridged complexes to induce a redox asymmetry to probe the degree of coupling between the metal centers.[21]

Oxidation of the binuclear complexes results in a decrease of ca. 50 cm^{-1} for the stretching vibration of the bridging cyano group of those compounds for which this band could be assigned.[9] This fact is in agreement with the participation of a π-bonding orbital of the bridging cyanide in the HOMO of the binuclear complex (Figures 3–6), since removal of an electron therefrom must produce a weakening of the CN bond strength. On the other hand, the changes observed in the ν(CO) frequencies when the complexes are oxidized clearly parallel the calculated increase in the net charges on the two Mn atoms upon the removal of an electron from the binuclear complexes (Table II). Thus, in those cases where the oxidation takes place in one trans-$Mn(CO)_2$ fragment, the computed charge of the Mn atom increases by ca.

(21) de la Rosa, R.; Chang, P. J.; Salaymeht, F.; Curtis, J. C. *Inorg. Chem.* **1985**, *24*, 4229.

0.6, and the corresponding ν(CO) frequency increases by ca. 70 cm^{-1}, while if the oxidation occurs on the other metal fragment (at the other side of the CN bridge) the charge is raised by ca. 0.2, and the increase of the stretching frequency is only 10 cm^{-1} (the average of the two strong ν(CO) absorptions of the cis fragments behaves similarly). However, there is not a simple direct relationship between the composition of the MO of the complexes and the variations in the ν(CO) frequencies.

The clear (though small) variations in $E°_1$ with the nature of the fragments at each side of the CN bridge of the binuclear complexes and the changes in the ν(CO) stretching frequencies in both fragments upon oxidation suggest some electronic communication between the two manganese atoms. Consistently, as mentioned above, the numerical results of our calculations suggest that the two $Mn(CO)_2$ sites are weakly coupled. The dications formed after the first oxidation can therefore be considered as class II mixed-valence complexes in the Robin and Day classification.[2] This is in agreement with the differences observed[9] between $E°_1$ and $E°_2$ for each complex, although no band assignable to the intervalence transfer absorption could be detected in the electronic spectra of the complexes.[22] The results of the ESR measurements[9] are also consistent with this general picture, in supporting the localization of the unpaired electron mainly on one of the two metal centers.

Finally, knowing the electronic structure of the complexes helps in an understanding of the observed oxidatively induced isomerization processes.[9,10] The main experimental observations are (i) when the oxidation affects a cis-dicarbonyl site, it is followed by a rapid isomerization of that site to the trans form, and (ii) the [trans–CN–cis]$^{2+}$ dications (**2**), for which the oxidation takes place at the trans site, spontaneously isomerize to [trans–CN–trans]$^{2+}$ at a rate that markedly depends on the monodentate ligand L coordinated to the *cis*-dicarbonyl moiety, being faster for better donor L ligands.

The isomerization of a cis site upon oxidation has been observed for the [cis–CN–trans]$^{+}$ isomer (**3**) after two one-electron oxidation steps. It is well-known that in the oxidized mononuclear dicarbonyl complexes the trans forms are thermodynamically preferred[23] and that the barrier for an octahedral → trigonal prism → octahedral isomerization pathway[24] decreases with electron configuration in the order $d^6 > d^5 > d^4$. Similarly, the oxidation of the octahedral tricarbonyls d^6-$M(CO)_3L_3$, gives the *mer* isomeric form, which is favored in the higher oxidation states, although recently the first example of a tricarbonyl species having equally stable *fac*- and *mer*-tricarbonyl oxidized species has been reported.[25] It is also believed that those isomerization processes consist of an intramolecular twist mechanism[26] that has a lower rotation barrier if the charge of the metal center is increased.

Since the oxidation of [trans–CN–cis]$^{+}$ (**2**) affects in part the cis site (Table II), the barrier for the octahedral–trigonal twist should be somewhat decreased, but the calculated barriers, 3.52 and 2.94 eV for the mono- and dications, respectively, are quite similar, suggesting that a different pathway for the isomerization must exist. An alternative mechanism consists in the excitation of an electron from xy^N (or yz^N) to the semioccupied HOMO (xy^C), formally an intramolecular oxidation of the N-bonded *cis*-$Mn^I(CO)_2$ fragment by the C-bonded *trans*-$Mn^{II}(CO)_2$ (see the calculated charges in Table II), which is akin to an inner-sphere oxidation mechanism. The isomerization of the oxidized Mn^N fragment can then proceed readily, as happens for other Mn^{II} compounds. The barrier for such electron-transfer processes can be estimated at the extended Hückel level from the energy difference between the two highest occupied orbitals (roughly 0.5 eV for compound **2**, Figure 4). In summary, both isomerization and electron-transfer processes occur and may be represented by the equation

$$[\text{trans-Mn}^{II}\text{-CN-cis-Mn}^{I}]^{2+} \rightarrow [\text{trans-Mn}^{I}\text{-CN-trans-Mn}^{II}]^{2+}$$

a process in which the isomerization is driven by the electron transfer, although the qualitative nature of our study does not allow us to draw definitive conclusions and further experimental data might be needed to fully understand these oxidatively induced isomerization processes.

As might be expected, it is observed that the isomerization process is easier in the cases where the redox potential of the C-bonded fragment is higher or where the redox potential of the N-bonded fragment is lower (i.e., when the difference between the redox potentials of the two fragments is smaller[9,10]). It is therefore clear that the rate of the isomerization can be finely modified by adjusting the redox potentials at each site of the bridge (by changing the ligands on each Mn), and therefore these complexes can be useful for the study of intramolecular electron transfer in asymmetrical systems.[27]

Notice that the orbital control of the oxidative isomerization allows us to attempt a fine-tuning of the isomerization rates. A calculation carried out on the model asymmetrical complex [*trans*-$P(OH)_3(PH_3)_2(CO)_2Mn$–CN–*cis*-$Mn(CO)_2(PH_3)_3]^{+}$ (**5**, Tables I and II) indicates that its HOMO has a larger contribution from frontier orbitals of the cis fragment than in the case of the analogous derivative with PH_3 as ligands. Consequently, the dication produced upon oxidation is more delocalized, and the increase in the charge of the cis-Mn site is more pronounced, thereby increasing the rate of the isomerization process.

Acknowledgment. The authors are grateful to the Spanish DGICYT for financial support (Projects PB88-0468 and PB89-0268), to the University of Oviedo for a short-term research grant to E.P.-C., and to the Spanish Ministerio de Educacion y Ciencia for an Acción Integrada grant.

(22) The UV/vis spectra of the mixed-valence dication {*trans*-[$P(OPh)_3$]-(dppm)$(CO)_2Mn$–CN–*trans*-$Mn(CO)_2$(dppm)[$P(OPh)_3$]}$^{2+}$ recorded in CH_2Cl_2 showed two intense absorptions at 436 (ϵ 2500) and 640 (ϵ 3850) nm and a very intense broad absorption in the UV region. The spectrum of the very freshly generated trication showed, in addition of the intense high-energy band, two bands at wavelengths almost identical to those of the dication, but with roughly double extinction coefficients, i.e. 440 (ϵ 3900) and 630 (ϵ 8500) nm, while the spectrum of the monocation showed only the intense and broad UV absorption with a shoulder at ca. 400 nm. Therefore, it appears that the spectrum of the dication is the simple addition of the contribution of one Mn(I) chromophore and one Mn(II) chromophore and does not include any feature that could be attributed to an IT absorption band.

(23) Geiger, W. E. *Prog. Inorg. Chem.* **1985**, *33*, 275.
(24) Hoffmann, R.; Howell, J. M.; Rossi, A. R. *J. Am. Chem. Soc.* **1976**, *98*, 2484.
(25) Bond, A. M.; Colton, R.; Feldberg, S. W.; Mahon, P. J.; Whyte, T. *Organometallics* **1991**, *10*, 3320.
(26) Bond, A. M.; Colton, R.; McDonald, M. E. *Inorg. Chem.* **1978**, *17*, 2842.
(27) Richardson, D. E. *Comments Inorg. Chem.* **1985**, *3*, 367.